Call: H2020-SC5-2014-two-stage
Topic: SC5-01-2014

PRIMAVERA
Grant Agreement 641727

PRocess-based climate sIMulation: AdVances in high resolution modelling and European climate Risk Assessment

Deliverable D*4.4*

Assess the representation of convection influences on the diurnal cycle phase and its impacts on land-surface-atmosphere fluxes, with potential implications for climate change impacts over Southern Europe. Use standard models with parameterised atmospheric convection, stochastic physics models and models with ~5km atmosphere resolution.

Deliverable Title	*Assess the representation of convection influences on the diurnal cycle phase and its impacts on land-surface-atmosphere fluxes, with potential implications for climate change impacts over Southern Europe. Use standard models with parameterised atmospheric convection, stochastic physics models and models with ~5km atmosphere resolution.*	
Brief Description	*Analyses of impact of increased resolution, stochastic physics and explicit deep convection on the phase and amplitude of the diurnal cycle of precipitation in a series of global climate model simulations*	
WP number	4	
Lead Beneficiary	*UOXF*	
Contributors	*Daniel J. Befort, University of Oxford* *Kristian Strommen, University of Oxford* *Hannah Christensen, University of Oxford* *Tim Palmer, University of Oxford* *Antje Weisheimer, University of Oxford* *Nils Wedi, ECMWF* *Peter Bechtold, ECMWF* *Malcolm Roberts, UK Met Office* *Mark Muetzelfeldt, University of Reading* *Reinhard Schiemann, University of Reading*	
Creation Date Version Number Version Date	May 2020 V2 May 2020	
Deliverable Due Date Actual Delivery Date	May 2020 May 2020	
Nature of the Deliverable	R	*R - Report*
		P - Prototype
		D - Demonstrator
		O - Other
Dissemination Level/ Audience	PU	*PU - Public*
		PP - Restricted to other programme participants, including the Commission services
		RE - Restricted to a group specified by the consortium, including the Commission services
		CO - Confidential, only for members of the consortium, including the Commission services

Table of Contents

1. Executive Summary

This deliverable presents the key outcomes regarding the representation of the amplitude and phase of the diurnal cycle of precipitation in a subset of PRIMAVERA simulations. Special emphasis is put on the impact of increased resolution, stochastic physics, and deep-convection parametrisation on the diurnal cycle characteristics.

It is found that the overall observed global pattern of the phase of the diurnal cycle is captured in the PRIMAVERA EC-Earth simulations, however, over both land and ocean grid cells the peak of precipitation occurs too early in the model. By comparing results for two EC-Earth simulations at standard low- (TL255) and high- (TL511) resolutions, it is found that the diurnal cycle phase is only marginally impacted by increased resolution. In contrast the diurnal cycle amplitude bias is reduced in the high-resolution experiment compared to the low-resolution experiment, even though the general difference pattern is apparent in both experiments.

The amplitude error in the 1st harmonic of diurnal cycle precipitation compared to observations is similarly reduced by either reducing the grid spacing from 80km (TL255) to 40km (TL511) or through the impact of stochastic physics applied in an 80km EC-Earth simulation, whereas the phase error is not affected by the usage of stochastic physics. The improvement for the amplitude adds to the scientific understanding of the positive impact of stochastic physics on mean state and variability presented in Deliverable D4.1.

The impact of deep-convection parametrisation has been tested using simulations conducted at 4km and 10km resolution using the ECMWF IFS and Met Office HadGEM3-GC31 models respectively. Comparing European summer rainfall in HadGEM3-GC31 at 10km resolution with parameterised convection (N1280) and in an experimental setup with explicit convection (N1280-EC) shows too frequent and too weak precipitation in N1280. Both frequency and intensity are better represented in N1280-EC overall, yet this is not reflected in a smaller mean bias. Switching off the parameterisation typically improves the phase of the diurnal cycle of precipitation over land, with rain coming somewhat later in the afternoon compared to when the parameterisation is used. This can be seen both globally, particularly over the tropics, as well as over Europe. However, there can also be significant changes to the global radiation budget with this change, indicating that the model may need extensive retuning, which is unsurprising given how critical the process of convection is to global climate.
ECMWF IFS experiments show that 4km resolution w/o deep convection improves the phase of the diurnal cycle, but results are far from converged and it is expected that 1 km grid spacing or less may be required to converge. Comparison with EC-Earth results suggest a resolution dependency of the diurnal cycle in IFS simulations with deep convection parametrisation on.

Finally, the relationship between future changes in precipitation and the diurnal cycle characteristics is assessed using EC-Earth. It is found that over most of the tropics land regions, except India, large parts of the projected total precipitation change are caused by a change of the diurnal cycle amplitude. However, the robustness of the results is hampered by the limited number of ensemble members used and the high influence of internal variability on near-term future precipitation changes. We also find that mean-state changes in heat fluxes and soil moisture correlate strongly with changes in precipitation, and these changes are therefore also closely related to changes in the diurnal cycle amplitude. Due to the fact that the diurnal cycle phase is not found to systematically change when including stochastic physics, or when increasing resolution to an extent which still does not resolve convection, diurnal cycle biases may influence future projections of important processes such as heat waves and droughts.

2. Project Objectives

With this deliverable, the project has contributed to the achievement of the following objectives (DOA, Part B Section 1.1) WP numbers are in brackets:

No.	Objective	Yes	No
A	To develop a new generation of global high-resolution climate models. *(3, 4, 6)*	X	
B	To develop new strategies and tools for evaluating global high-resolution climate models at a process level, and for quantifying the uncertainties in the predictions of regional climate. *(1, 2, 5, 9, 10)*	X	
C	To provide new high-resolution protocols and flagship simulations for the World Climate Research Programme (WCRP)'s Coupled Model Intercomparison Project (CMIP6) project, to inform the Intergovernmental Panel on Climate Change (IPCC) assessments and in support of emerging Climate Services. *(4, 6, 9)*		X
D	To explore the scientific and technological frontiers of capability in global climate modelling to provide guidance for the development of future generations of prediction systems, global climate and Earth System models (informing post-CMIP6 and beyond). *(3, 4)*	X	
E	To advance understanding of past and future, natural and anthropogenic, drivers of variability and changes in European climate, including high impact events, by exploiting new capabilities in high-resolution global climate modelling. *(1, 2, 5)*	X	
F	To produce new, more robust and trustworthy projections of European climate for the next few decades based on improved global models and advances in process understanding. *(2, 3, 5, 6, 10)*		X
G	To engage with targeted end-user groups in key European economic sectors to strengthen their competitiveness, growth, resilience and ability by exploiting new scientific progress. *(10, 11)*		X
H	To establish cooperation between science and policy actions at European and international level, to support the development of effective climate change policies, optimize public decision making and increase capability to manage climate risks. *(5, 8, 10)*		X

3. Detailed Report

In-depth analyses are carried out on a series of global climate model simulations, mainly conducted within PRIMAVERA, to assess the impact of increased resolution, stochastic physics and explicit deep convection on the phase and amplitude of the diurnal cycle in precipitation. All datasets used for this report are listed in Table 1.

Depending on the dataset, calculations are either performed using hourly data as e.g, for 4km ECMWF simulations or using 3 hourly data. TRMM 3B42 (Huffman et al., 2007) 3 hourly observational data is used as reference except if stated otherwise. For all analyses, except those presented in Section 3.1.3 using data from the Met Office and ECMWF IFS, the input data has been interpolated to a common 1x1 degree grid.

The phase and amplitude of the first harmonic of the diurnal cycle of precipitation is calculated by applying a Fast-Fourier-Transformation (fft) on the long-term average sub-daily precipitation amounts. Next, the phase is further transformed from UTC into local time (LT), by using the following equation:

LT = UTC + (longitude of location)/15

Besides analysing the diurnal cycle using a fft approach, the daily precipitation cycle is assessed separately for several regions: Southern Europe (35N-45N, 10W-40E), the tropics (20S-20N) and the Amazon (15S-0S, 80W-50W). Analyses are mainly carried out for the boreal summer season June-July-August (JJA).

Due to a bug in the cmorization tool, time bounds have been set incorrectly for the PRIMAVERA EC-Earth data used in this study, which is related to the report at https://github.com/EC-Earth/ece2cmor3/issues/354. Thus, 3-hourly data from EC-Earth simulations at 0,3,6,9,12,15,18,21 UTC represent the *start* of the averaging period. Here, we associated the precipitation during e.g. 0 and 3UTC to 1.5UTC and so on.

3.1 Phase and amplitude of the diurnal cycle of precipitations

3.1.1 Impact of increased resolution

To assess the impact of increased resolution on the diurnal cycle characteristics (phase and amplitude) two model simulations using EC-Earth with different resolutions but otherwise with identical setup are used (see Table 1). This includes an EC-Earth simulation at TL255 (~ 80km grid-spacing at the equator), EC-Earth-LR, and at TL511 (~ 40km grid-spacing at the equator), EC-Earth-HR, which both cover the time period from 2000 until 2014.
Figure 3.1.1 shows the phase of the diurnal cycle for TRMM observations, EC-Earth LR and EC-Earth HR. In observations a strong land-sea contrast is found, with the maximum of the diurnal cycle over land occurring during the late afternoon and evening hours, whereas over oceans the diurnal cycle peaks in the early morning hours. EC-Earth is able to reproduce this general pattern as outlined first by Bechtold et al. (2014), however, there are some differences to observations. For both EC-Earth simulations the diurnal cycle peaks too early, which is especially pronounced over the Amazon. This is further confirmed by Figure 3.1.2, which illustrated the distribution of the maximum of the diurnal cycle over all ocean and land grid cells within the tropical band (20S-20N). For most land points the peak of the diurnal cycle occurs between 18 and 00 LT, whereas for EC-Earth-LR it is found around 18 hours LT. The results are similar for ocean grid cells, for which the peak is observed between 3 and 8 hours LT whereas the peak is much more pronounced and centred around 3 hours LT for EC-Earth. The diurnal cycle characteristics are similar for EC-Earth HR, however, here the peak of the diurnal cycle over land and ocean points in the tropics is even earlier than in EC-Earth LR.

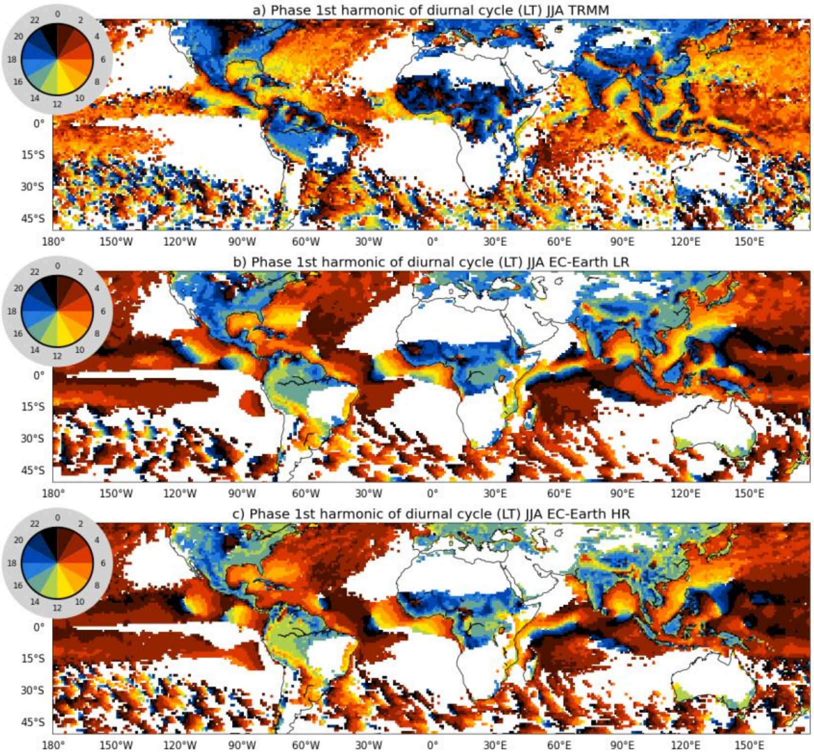

Figure 3.1.1 Phase of 1st harmonic of diurnal cycle of precipitation for a) TRMM 3B42 observations, b) EC-Earth-LR and c) EC-Earth-HR in local time (LT) calculated using data from 2000 until 2014. Areas for which amplitude is below 0.2 are masked.

The amplitude of the first harmonic in TRMM observations resembles the total precipitation pattern, with high amounts over the tropics and generally smaller amounts over the extra-tropics (Fig. 3.1.3a). This general pattern is well simulated by EC-Earth, however local differences between modelled and observed values are large. In general, both EC-Earth LR and EC-Earth HR overestimate the amplitude over most parts of the tropics, except over the Indian subcontinent (Fig. 3.1.3b&c). Differences in the amplitude of the diurnal cycle are reduced in EC-Earth-HR., e.g. over the Maritime Continent, which might have implications for the propagation of the MJO across this region.

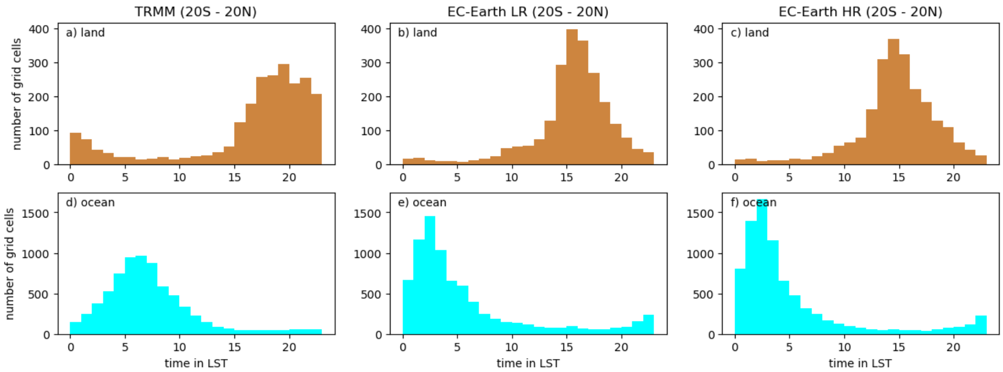

Figure 3.1.2 Histograms of phase of first harmonic of the diurnal cycle (time given in LT) for grid cells in the tropical band (20S-20N) for TRMM (a & d), EC-Earth-LR (b & e) and EC-Earth-HR (c & f). Top row: land and bottom row for ocean grid cells. Only grid cells with amplitudes larger than 0.2mm are take into account.

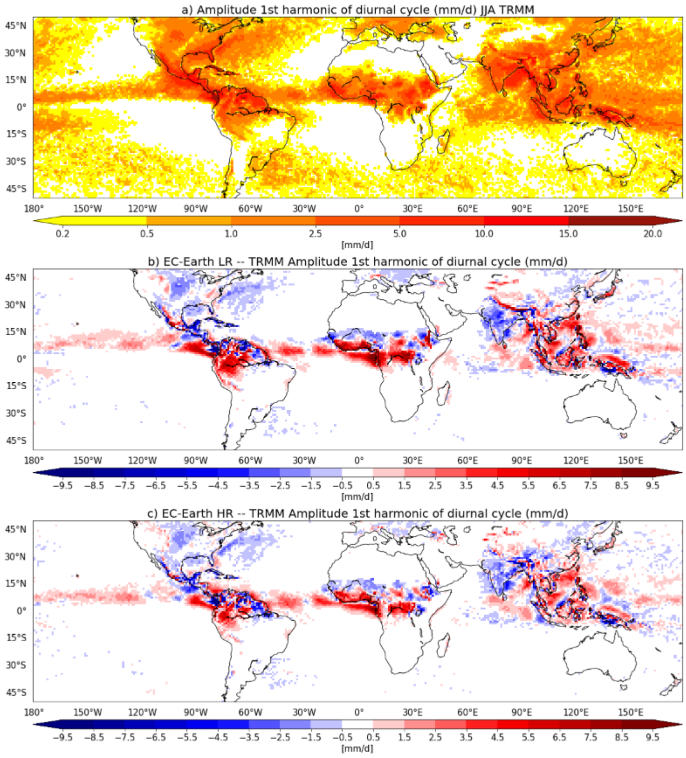

Figure 3.1.3 Amplitude of 1st harmonic of diurnal cycle of precipitation for a) TRMM 3B42 observations, b) Difference between EC-Earth LR to TRMM and c) Difference between EC-Earth HR and TRMM calculated using data from 2000 until 2014. Areas for which amplitude is below 0.2 are masked

3.1.2 Impact of stochastic physics

Within PRIMAVERA, EC-Earth simulations w/ (EC-Earth SP) and w/o stochastic physics (EC-Earth no-SP) have been conducted (Table 1). Except for stochastic physics being turned on, these simulations share an identical setup with both being conducted in low resolution TL255. The configuration of stochastic schemes in the experiment considered is as follows: in the atmospheric component the Stochastically Perturbed Parameterisation Tendencies (SPPT) scheme is used (Buizza et al., 1999; Palmer et al., 2009). In the land-scheme (H-Tessel) of EC-Earth the Stochastic Land scheme described in Strommen et al. (2019) is activated, and in the ocean component (NEMO) the schemes described in Juricke et al. (2014) and Juricke et al. (2017) are activated. Thus, the simulation EC-Earth SP has a stochastic component added to all the major parts of the model physics, including both tendency and parameter perturbations.
The only difference between the EC-Earth simulation w/o stochastic physics (EC-Earth No-SP) used in this analysis and the low-resolution EC-Earth LR simulation used in Section 3.1.1 is that the model simulation has been conducted on a different high-performance computer. Thus, the simulated phase of the first harmonic of both simulations shows only small differences (compare Fig 3.1.4a and 3.1.1b). Furthermore, it is found that including stochastic physics does affect the diurnal cycle phase only to a small extend (Fig. 3.1.4b).

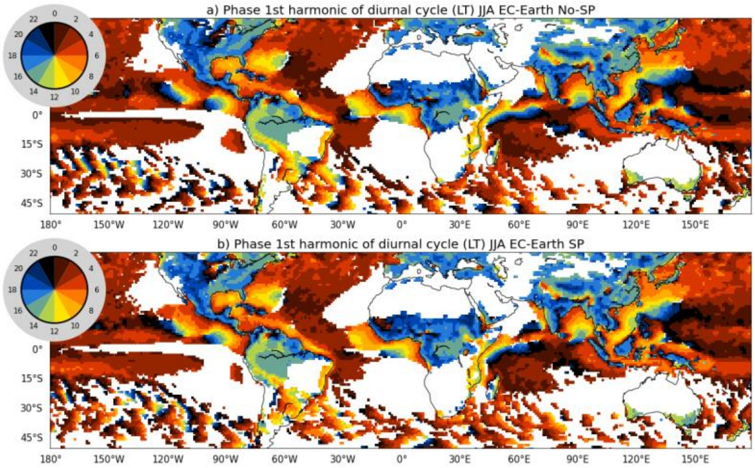

Figure 3.1.4 Phase of 1st harmonic of diurnal cycle of precipitation for a) EC-Earth no-SP and b) EC-Earth SP in local time (LT) calculated using data from 2000 until 2014. Areas for which amplitude is below 0.2 are masked.

Larger impact of stochastic physics is found for the amplitude of the first harmonic of the diurnal cycle (Fig. 3.1.5). Even though both simulations tend to overestimate the amplitude over large parts of the tropics (except India), the biases are smaller for EC-Earth SP simulation compared to EC-Earth No-SP. This is very similar to the result obtained for increased resolution, for which the amplitude biases are decreased in EC-Earth HR compared to EC-Earth LR. This suggests that the usage of stochastic physics in climate simulations can be beneficial to reduce biases of the amplitude of the diurnal cycle. The reader is further referred to results presented in PRIMAVERA Deliverable D4.1, showing that stochastic physics can lead to broad improvements in the model mean and variability.

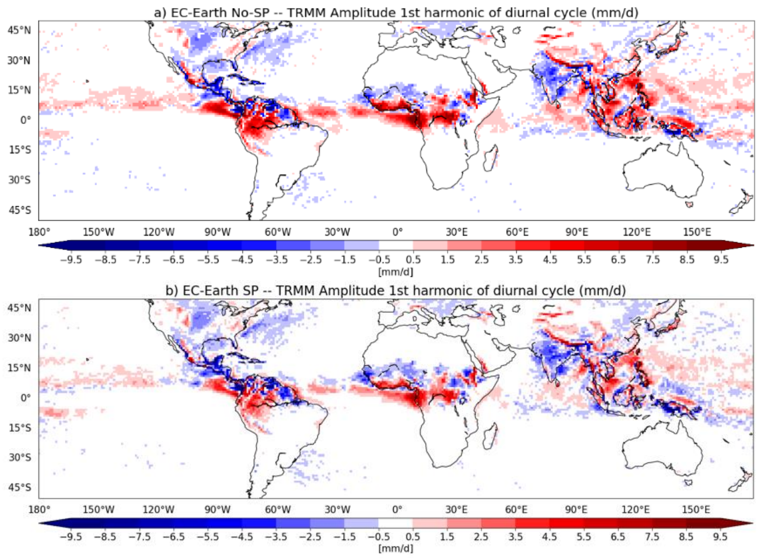

Figure 3.1.5 Differences in amplitude of 1st harmonic of diurnal cycle of precipitation to TRMM observations for a) EC-Earth No-SP and b) EC-Earth SP calculated using data from 2000 until 2014.

3.1.3 Impact of deep-convection parameterization

To assess the impact of the deep convection parametrisation on the diurnal cycle of precipitation, several high-resolution simulations have been conducted using ECMWF IFS model and HadGEM3-GC31 (see Table 1).

Results using ECMWF IFS model

The impact of high resolution and the deep convection parametrisation on the diurnal cycle has been assessed with the latest operational version 2019/2020 of the ECMWF IFS model. Daily 48h re-forecasts for August 2016 have been run w/ and w/o the deep convection parametrisation at 4 km horizontal resolution, the total precipitation fields were archived hourly and the diurnal cycle analysis was done considering only the 24-48 forecast range. A 1-month dataset only allows for robust diurnal cycle statistics in the tropical regions but not for the middle latitudes which are dominated by synoptic variability. Ideally, the analysis should be extended for a whole or several summer seasons, but this was not possible due to computational and archiving constraints.

The diurnal phase of precipitation from the reforecast w/ and w/o the deep convection scheme and their difference are displayed in Figs 3.1.6. Several important remarks can be made. In w/o the diurnal cycle over tropical Africa, South America, South-East Asia and southern North America occurs typically 2-4 h later than in w/ and is in better agreement with the observations in Figure 3.1.6a. The diurnal cycle in the 4km resolution w/ simulation also occurs roughly 2 hours earlier than in the lower resolution EC-Earth runs (Figures 3.1.1). Therefore, the convection parametrisation exhibits also a resolution dependency with a diurnal cycle that is shifted from the late afternoon hours (as observed) in the low-resolution EC-Earth run to the early afternoon hours in the 4 km ECMWF IFS run.

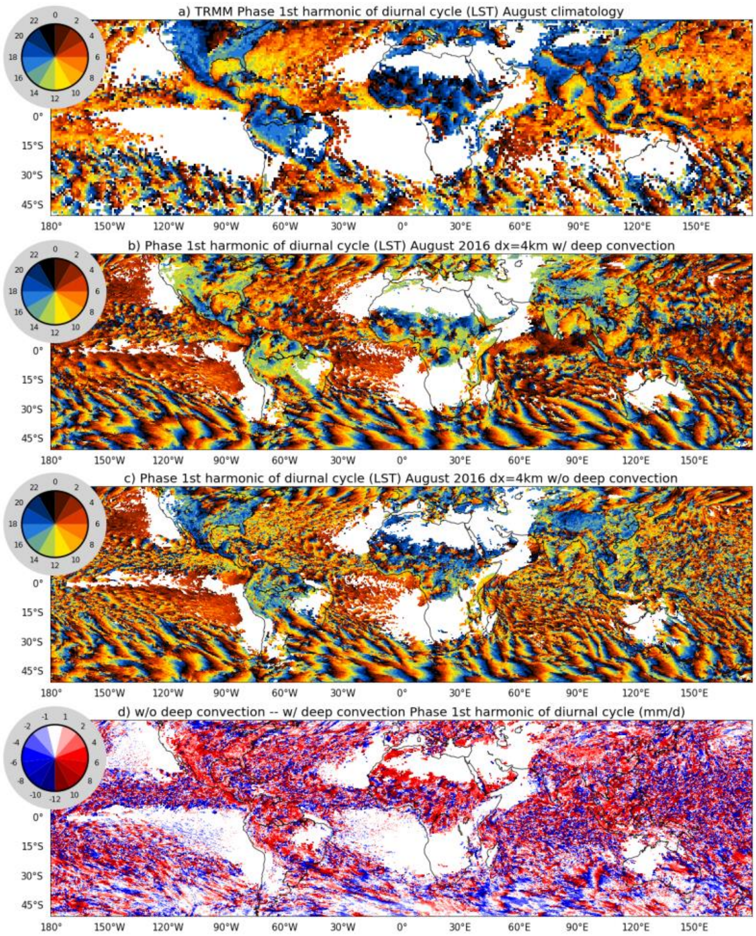

Figure 3.1.6 : Phase of 1st harmonic of diurnal cycle of precipitation for a) TRMM 3B42 observations, b) ECMWF IFS w/ deep convection, c) ECMWF w/o deep convection and d) difference between ECMWF IFS w/o deep convection and ECMWF IFS w/ deep convection in local time (LT). For TRMM 3 hourly precipitation for August from 2000 until 2014 is used, whereas the phase for IFS experiments is calculated using hourly August precipitation data from 2016 only. Areas for which amplitude is below 0.2 are masked.

However, a more differentiated picture is obtained from the histograms of phase in Figure 3.1.7. The 4 km run w/o starts even earlier during the day than the w/, both exhibit a maximum around 15 LST, but while the rainfall in the w/ simulation drops off quickly the w/o has a secondary maximum during the late evening/night

Overall the 4 km w/o deep convection more realistically represents the diurnal phase of the precipitation as it has a reduced daytime peak and more night-time precipitation than w/. However, it overestimates the predicted precipitation by 10-20%. One should also keep in mind that explicit simulations of deep convection exhibit itself a very strong resolution dependency by strongly delaying the onset of convection (condensation) for resolutions >5 km. A convergence of the numerical results (phase and intensity of the convection) is only expected with horizontal resolutions of O(1 km) (Yashiro et al. 2016.; Sato, 2008; Love et al., 2011; Jin et al., 2016).

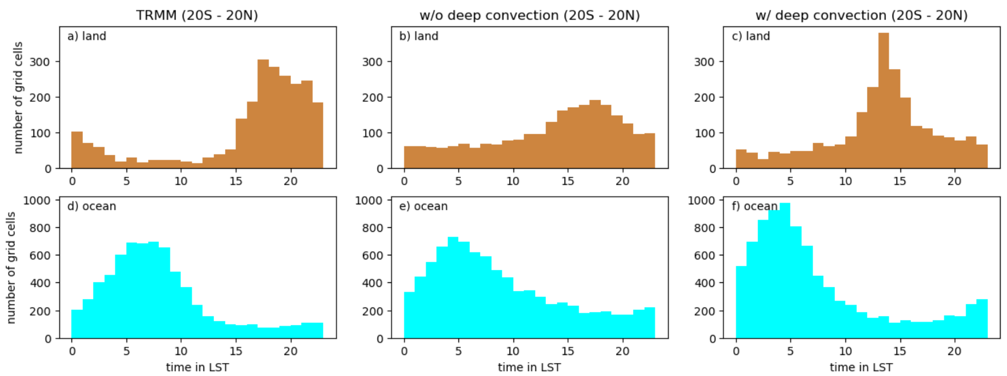

Figure 3.1.7 Histograms of phase of first harmonic of the diurnal cycle (time given in LT) for grid cells in the tropical band (20S-20N) for TRMM (a & d), ECMWF w/o deep convection (b & e) and ECMWF w/ deep convection (c & f). Top row: land and bottom row for ocean grid cells. Only grid cells with amplitudes larger than 0.2mm are take into account.

Results using HadGEM-GC3.1

Observations datasets used are: CMORPH (1998-2018), available up to 60°N at 30min frequency, and has been regridded to the N1280 model grid; TRMM (1999-2010), available up to 50°N at 3 hr frequency; and GPM (2015-2019), available up to 60°N at 30min frequency. It should be noted that using explicit convection at the 10km scale is rather unrealistic – this requires the model to uplift a whole gridbox column of air when convection takes place, not at all like the much smaller scales on which real convection happens. However, as a sensitivity study it still has value to suggest where convection schemes have problems, and what the consequences of these problems may be for the climate simulation.

More detail of the explicit convection setup can be found in Field et al. (2018). Similar simulations, with an older model configuration, and analysis can be found in Birch et al. (2015).

Mean properties of precipitation

The mean amount, frequency and intensity of summer rainfall over Europe from CMORPH and the parameterised (N1280) and explicit (N1280-EC) convection simulations are shown in Fig. 3.1.8 The N1280 simulation tends to have too frequent rainfall compared to CMORPH, but with much less intensity, which together combine to give a mean amount that is comparable to the observations.

For N1280-EC the frequency is somewhat improved, being less over much of Europe with a peak over the mountains. The intensity is also generally improved over land, but becomes rather more extreme over the Mediterranean than observed, and is too weak over the UK, the Atlantic and North Sea. These combine to give a mean amount which is rather too small over much of Europe, and possibly too enhanced over the mountains.

These figures show that care should be taken when comparing mean amounts of precipitation, since the mean value may agree with observations but be a combination of compensating errors in the various processes.

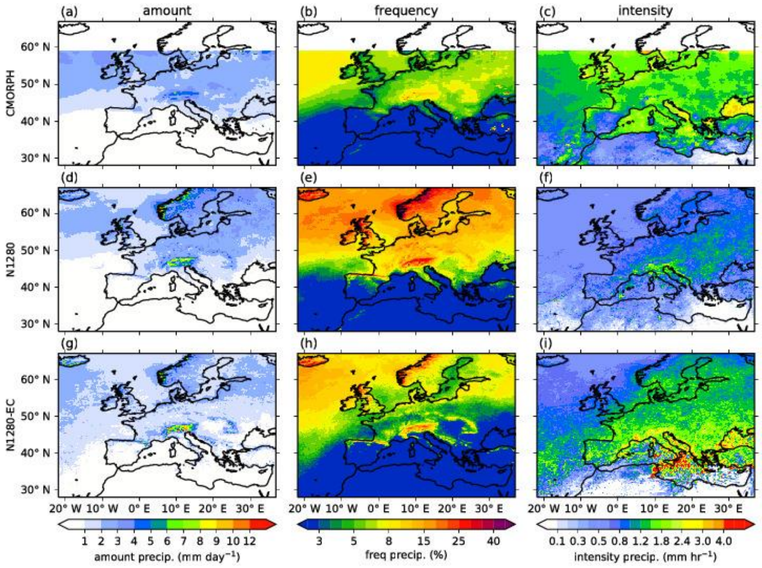

Figure 3.1.8 The mean JJA precipitation amount, frequency and intensity over Europe from CMORPH observations and model simulations with and without convective parameterisation (N1280 and N1280-EC respectively).

Phase of diurnal cycle over Europe

The phase of the diurnal cycle (DC) of precipitation, indicating the local solar time of peak precipitation, is shown in Fig. 3.1.9, again split into the mean precipitation, its frequency and intensity. The N1280 simulation has a DC which peaks too early in the day, typically around noon or earlier in Northern Europe, slightly later in Southern Europe. Together with this, the frequency peaks almost uniformly around noon, while the intensity peaks strongly close to midnight over central and eastern Europe. However, since the intensity in N1280 does not contribute strongly to the mean amount (Fig. 3.1.8f), the shift in the phase of the amount is not very strong.

For N1280-EC, the phase of the frequency is slightly later in the day than N1280, particularly near mountains or coastlines, though also weaker over some inland regions. The intensity is quite noisy, though values of late afternoon to midnight have a similar range to the observations over land and contrast with values of noon or earlier over much of the Mediterranean. These combine to give an amount that approaches the observed values.

To illustrate some of the uncertainties between different observational products, and to include an additional simulation, Fig. 3.1.10 shows the mean diurnal cycle including N1280-ED (explicit deep convection only), and TRMM and GPM observations. The differences between observations are relatively small compared to the model biases, with small differences in Eastern Europe and over the UK. The explicit deep simulation N1280-ED has some regions, often near coasts or mountains, with a slightly earlier peak than N1280-EC, but is generally closer to this simulation than N1280, suggesting that even over Europe the precipitation from deep convection is the main driver of the diurnal cycle.

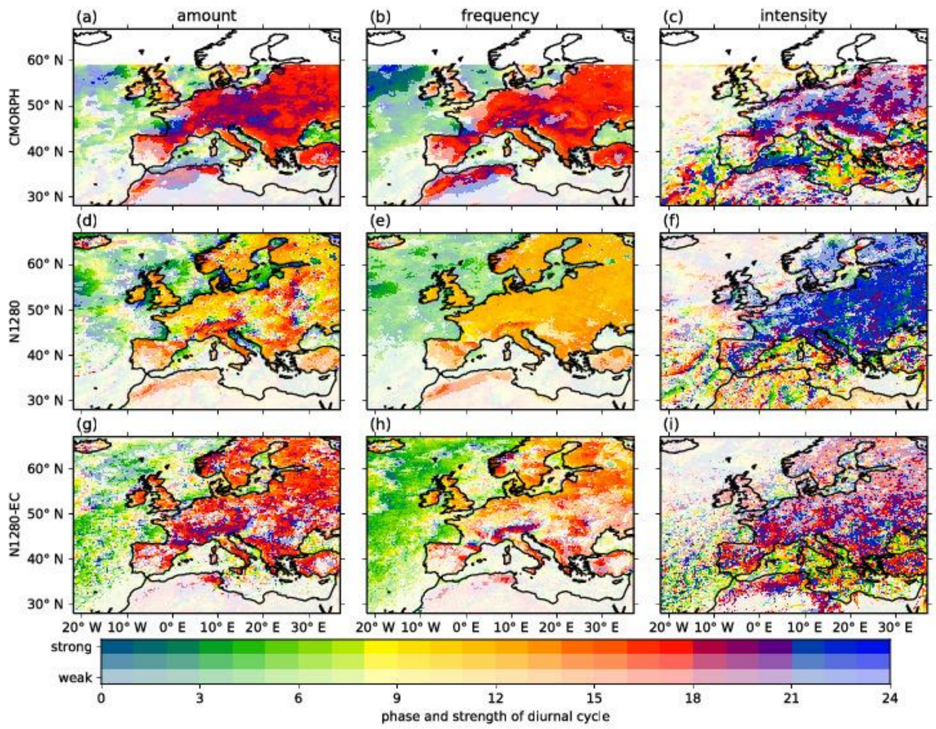

Figure 3.1.9 The diurnal cycle of JJA precipitation amount, frequency and intensity over Europe from CMORPH observations and model simulations with and without convective parameterisation (N1280 and N1280-EC respectively).

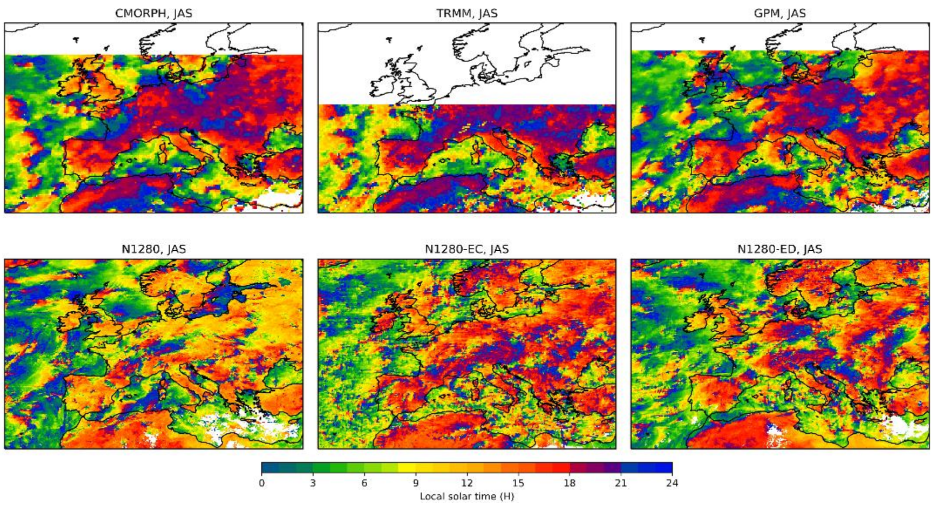

Figure 3.1.10 Phase of diurnal cycle of peak precipitation (local solar time) for observations and HadGEM3-GC31 models over July-August-September (JAS).

Global radiation balance

Ideally, given the change in diurnal cycle simulated, one would examine how this might impact on the global radiation budget and potentially local processes – if rainfall happens later in the day, this would impact the daily radiation budget, the surface conditions at the end of the day (soil moisture, temperature), and potentially other aspects.

We may anticipate that changes to the representation of convection may also change the global radiation balance of the model, due both to large-scale changes (for example clouds) and potential impacts of the diurnal cycle changes themselves.

Fig. 3.1.11 shows the globally averaged radiation components, and the global surface temperature, from the three different model simulations, both as monthly means and as a long-

term mean. It is immediately noticeable that the N1280-EC model has a dramatically different Top of Atmosphere radiation balance (TOA), with this model losing 7-8 W/m2 more heat from the climate system than the other two simulations. There are contributions to this from both an increase in Outgoing Shortwave (OSR) and (a slightly larger) contribution from Outgoing Longwave (OLR).
The explicit convection simulation has much less high thin and medium cloud, and a much warmer upper troposphere, together with changes to humidity and cloud ice. These elements combine to greatly change the radiation balance. Such a large imbalance in the radiation budget makes it difficult to interpret any surface changes in energy budget. Considerable tuning of this simulation would be needed in order to make progress on understanding process changes.

The explicit deep simulation has a smaller change in radiation budget from the parameterised run, and hence there is more potential for detailed comparison of the surface changes in this simulation. That is a target of future work.

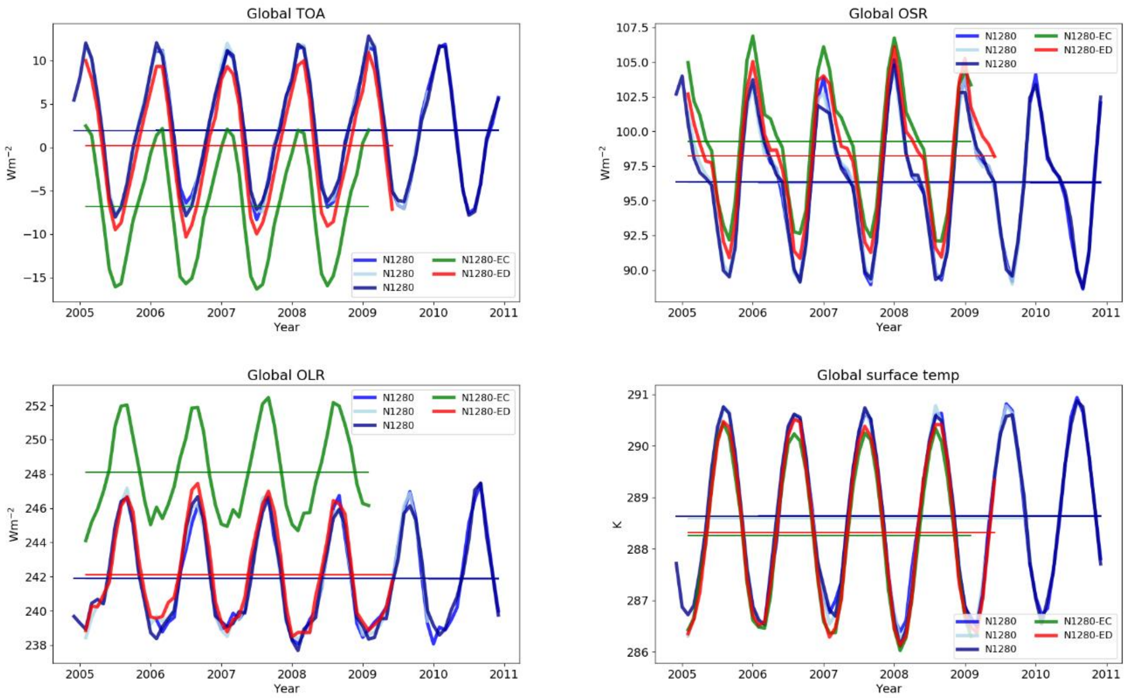

Figure 3.1.11 Global radiation budgets of the model simulations: Top of Atmosphere radiation (TOA), Outgoing Shortwave Radiation (OSR), Outgoing Longwave Radiation (OLR), surface temperature (ST). The mean values of the monthly timeseries curves are shown as straight lines.

3.2 Regional analyses of precipitation diurnal cycle

We now turn to considering aggregate changes across specific regions. We will look at the Tropics as a whole, the Amazon region and Europe, with a specific focus on Southern Europe. To compute the diurnal cycle across a full day, we compute, for each of the eight 3-hourly daily steps (00:00, 03:00, 06:00, …, 21:00), the mean precipitation across all such steps. This gives, for any grid point, a `3-hourly climatology’ which captures the full diurnal cycle at 3-hourly temporal resolution. Each grid point first has its timezone corrected to local time: the cycle of 3-hourly intervals produced is then interpolated back to the canonical steps (00:00, 03:00, …), prior to averaging over all gridpoints in the region.

The diurnal cycle of precipitation over the whole tropics land points (Fig. 3.2.1 left) shows huge differences between TRMM and the 3 EC-Earth simulations (EC-Earth No-SP, EC-Earth SP, EC-Earth HR). As already discussed, the maximum of the diurnal cycle is too early in all simulations but especially in the high-resolution experiment (see section 3.1 and Fig. 3.2.1 left). Large differences between the experiments are also found for the amplitude, which is overestimated especially by the low-resolution experiment and improved when using higher resolution or stochastic physics. Despite differences in the peak rainfall time, the models underestimate precipitation during the night (0 to 3 LT).

Differences between the model and observations are particularly large over the Amazon region and major improvements of the phase of the diurnal cycle are neither visible when using higher resolution nor when using stochastic physics (Fig 3.2.1 middle). However, slight improvements for EC-Earth HR and EC-Earth SP are found compared to the low-resolution EC-Earth No-SP simulation with regards to the amplitude of rainfall over the Amazon.
Aggregated over Southern Europe the models differ even more drastically to observations. The peak is again simulated too early in all EC-Earth experiments but especially in EC-Earth HR (Fig. 3.2.1 right). Furthermore, the minimum rainfall is simulated around midnight LT, whereas it is observed in the morning (around 9 LT) in TRMM data. Neither increased resolution nor stochastic physics do have a strong impact on the amplitude of the diurnal cycle and also limited impact on the phase. However, higher resolution and stochastic physics clearly impacts the mean state with increased average precipitation over Southern Europe compared to lower resolution.

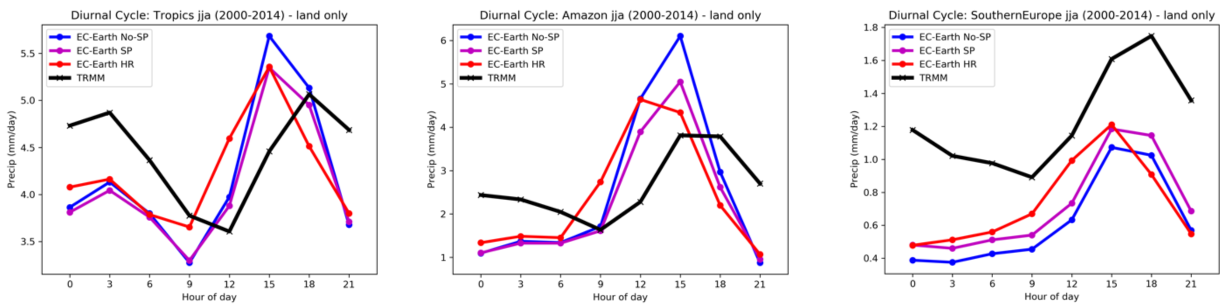

Figure 3.2.1 Climatological 3-hourly rainfall in TRMM observations and three EC-Earth simulations in LT for a) the whole tropics, b) the Amazon and c) Southern Europe. Only land grid cells are considered.

3.3 Future changes of diurnal cycle of precipitation and land-surface-atmosphere fluxes

Previous studies suggested that regional precipitation characteristics might undergo large changes under future climate change. The set of EC-Earth simulations is used to assess the extent to which total precipitation changes are related to changes in the amplitude of the diurnal cycle, and if the phase of the diurnal cycle is projected to change.
Projected change of the phase of the diurnal cycle are small and no large coherent patterns with robust changes are found (see Fig 3.3.1a for EC-Earth No-SP). This is different for projected changes in the amplitude of the diurnal cycle. Here, over most parts of the tropics the amplitude is projected to decrease (Fig 3.3.1b). This decrease can be explained not only by a decrease of precipitation during the peak hours but also due to an increase in precipitation during the night for which all experiments simulate small rainfall amounts (Fig 3.3.2). For the low-resolution EC-Earth No-SP experiment and EC-Earth HR experiment, total changes over the tropics are small. As the diurnal cycle amplitude is changing, this means that the same precipitation is spread more over the course of the day compared to under historical climate

conditions. In contrast, over the tropics, increased total precipitation is found for the stochastic experiment combined with a smaller amplitude under future climate conditions. Since both deterministic and stochastic experiments had similar performance in the historical period, but diverge in the future, we may conclude that there is enhanced uncertainty in projected Tropical precipitation changes. Because the stochastic experiment shows a different response to the high-resolution experiment, with both trying to represent sub-grid scale variability, this uncertainty is potentially associated with that coming from this unresolved variability.

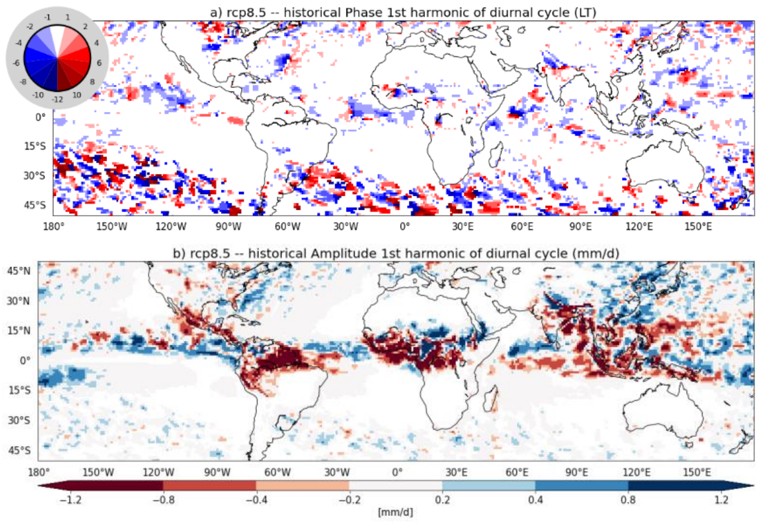

Figure 3.3.1 a) Projected future changes in the phase of the JJA diurnal cycle as derived from EC-Earth No-SP. b) same as a) but for projected changes in amplitude. 2000 to 2014 is used for the historical period and 2030 to 2049 for the future period.

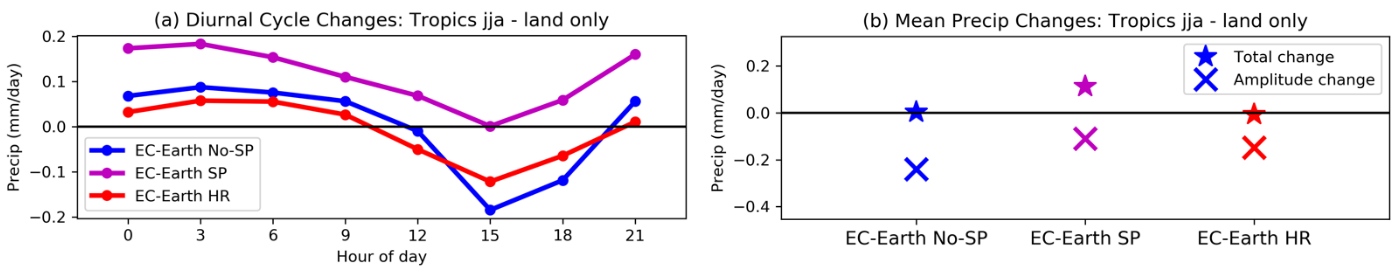

Figure 3.3.2 Future change to the diurnal cycle over the Tropics. a) future changes of sub-daily precipitation amounts (given in LT). b) Total averaged daily precipitation future change (star) and future change in amplitude (maximum – minimum). All for boreal summer (JJA).

However, the proportion to which changes in the diurnal cycle contribute to overall precipitation changes differs regionally. Over the Amazon both low-resolution experiments (w/ and w/o stochastic physics) do show a strong future change in the diurnal cycle as peak precipitation is decreased compared to the historical period (Fig 3.3.3). In contrast to the whole tropics the minimum precipitation during the night is only slightly changed over the Amazon. This means that large proportions of the total future precipitation change are due to a change in amplitude over this region. In contrast to both low-resolution experiments, no such change in the peak rainfall is found for the high-resolution experiment.

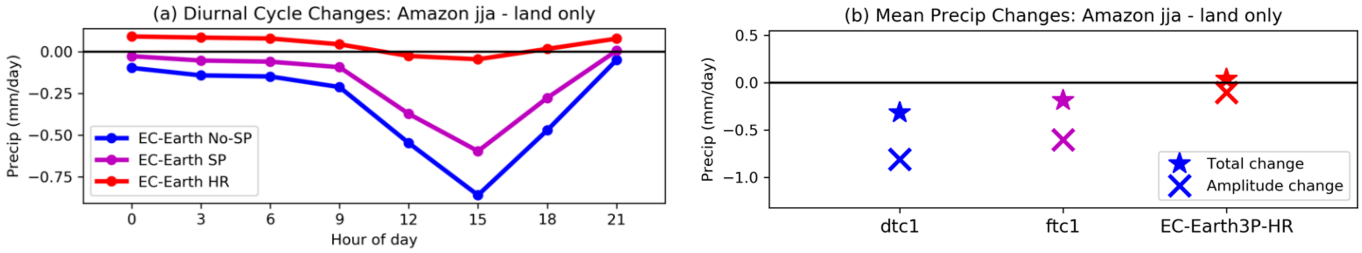

Figure 3.3.3 Same as Fig 3.3.2 but for the Amazon region

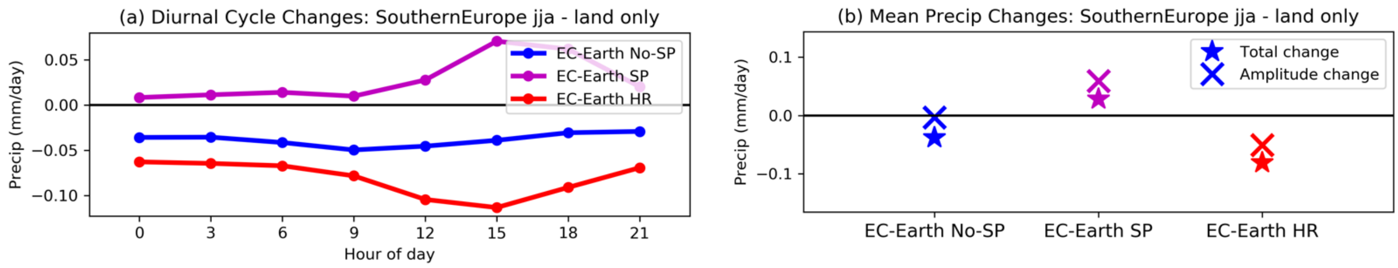

Figure 3.3.4 Same as Fig. 3.3.2 but for Southern Europe.

No consistency is found for the three EC-Earth experiments over Southern Europe, with no changes in total precipitation and also amplitude for EC-Earth No-SP, slight positive changes for EC-Earth SP and negative changes for EC-Earth HR (Fig 3.3.4). The inconsistency of the change, compared with the fact that both EC-Earth HR and EC-Earth SP both somewhat improved the total precipitation in the historical period (c.f. Figure 3.2.1), is again indicative of considerable uncertainty in these future projections.

Comparing future amplitude and future overall changes on a global scale shows that for the EC-Earth No-SP simulation, total precipitation changes over tropical land regions are to a large amount related to changes in amplitude, e.g. over the Amazon but also over western Africa and central America (Fig. 3.3.5). In contrast, precipitation changes over Asia and India seem to be less related to changes in the diurnal cycle amplitude. Precipitation changes for the high-resolution experiment indicate small changes over the Amazon, whereas over western Africa changes are more pronounced. The latter changes are to a large extent related to changes in the amplitude of the diurnal cycle. Total future precipitation changes over Asia and India are to a smaller extent related to changes in the diurnal cycle amplitude, which is in agreement with EC-Earth No-SP.

Over Europe the low-resolution EC-Earth No-SP experiment projects a drying over northern and central Europe and slight wetter conditions over parts of southern Europe (Fig. 3.3.6). These overall precipitation changes are only partly related to changes in amplitude. For the high resolution experiment the total precipitation change pattern differs, however, most changes are not related to changes in the diurnal cycle. Over Southern Europe in particular we find that for the stochastic and high-resolution experiment, the projected mean state change is to some extend driven by a change in the amplitude, though the sign of the change is opposite for the two experiments, with the high resolution experiment projecting an overall drying.

Figure 3.3.7 shows changes to upper level soil moisture in the future projections, with Figure 3.3.8 showing the same but restricted to Southern Europe only. We find broad agreement between soil moisture changes and precipitation changes (as shown in figures 3.3.5 and 3.3.6), with regions of increasing (decreasing) soil moisture corresponding to regions with increased (decreased) precipitation. In Figure 3.3.9 we also show sensible heat flux changes for Southern Europe, showing again a consistent response. Because changes in mean precipitation are accounted for by changes in the diurnal cycle for some key regions (including Southern Europe for some of the experiments), this implies that the future response for soil moisture and heat fluxes are likely strongly coupled to changes in the diurnal cycle. We showed that one cannot expect major changes to the representation of the diurnal cycle with stochastic physics or with an increase of resolution from about 80km to 40km. Indeed, improvements in the cycle were only found in models where the convection scheme was turned off. This suggests that future projections of processes driven by heat fluxes, precipitation and soil moisture (such as heat waves and drought) may be influenced by model biases in the representation of the diurnal cycle and that these biases cannot necessarily be expected to be notably reduced without moving to convection-permitting resolutions and/or improving the parameterisations.

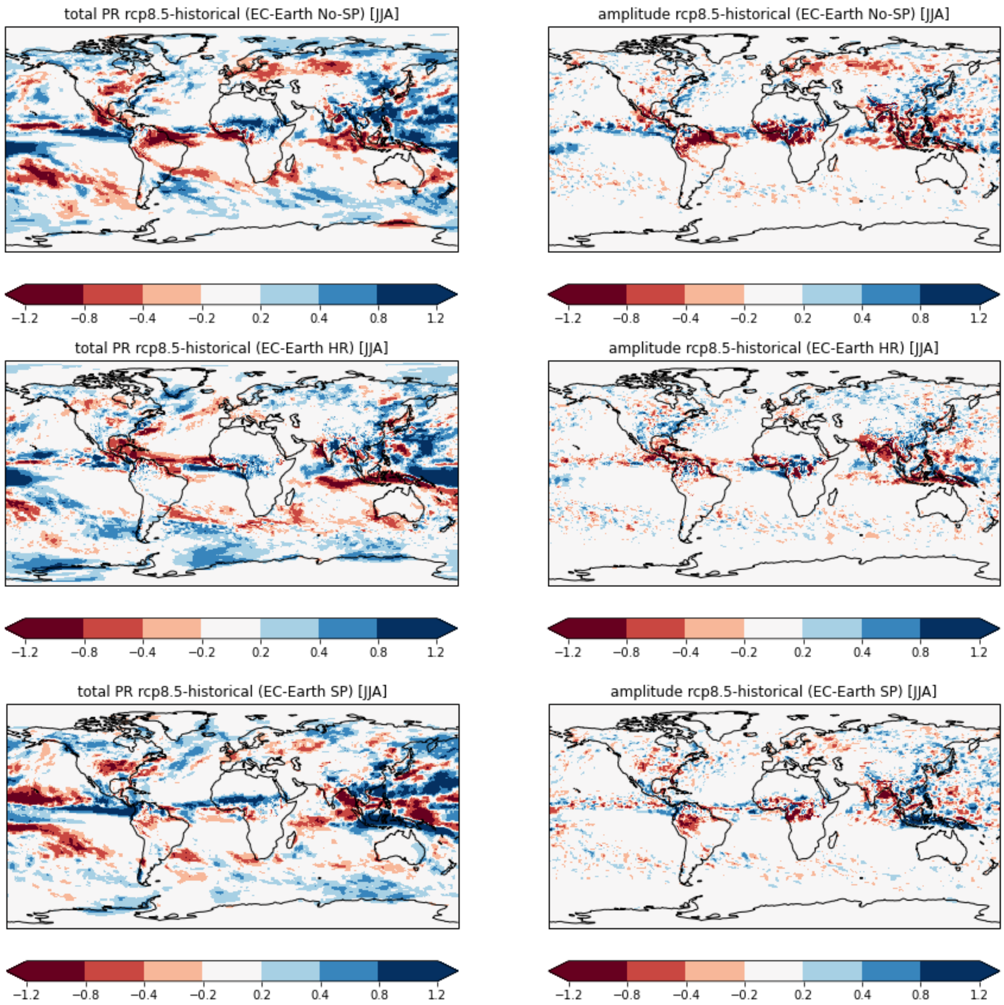

Figure 3.3.5 Future changes to mean precipitation (left column: total; right column: amplitude). JJA only. Top: EC-Earth No-SP, Middle: EC-Earth HR, Bottom: EC-Earth SP.

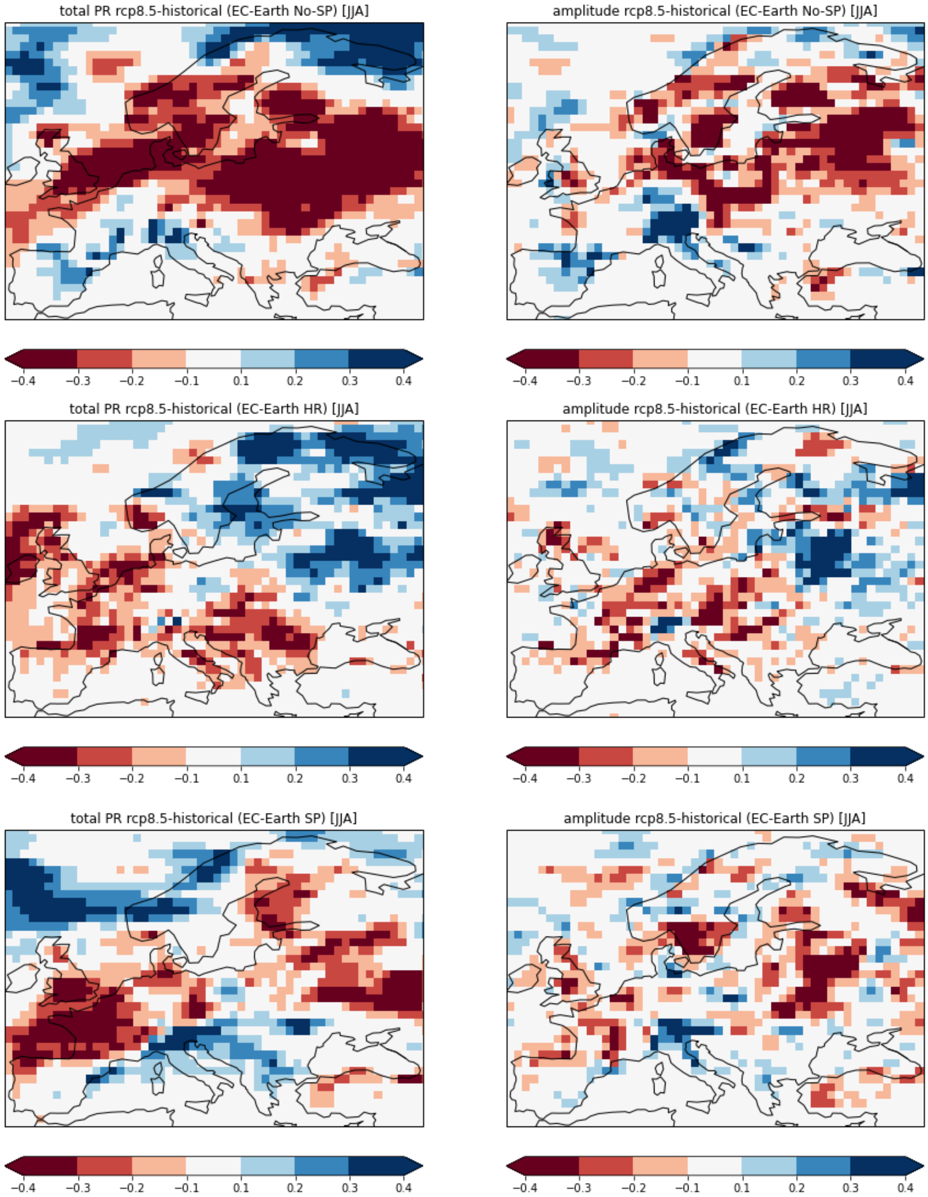

Figure 3.3.6 Same as 3.3.5 but for European region.

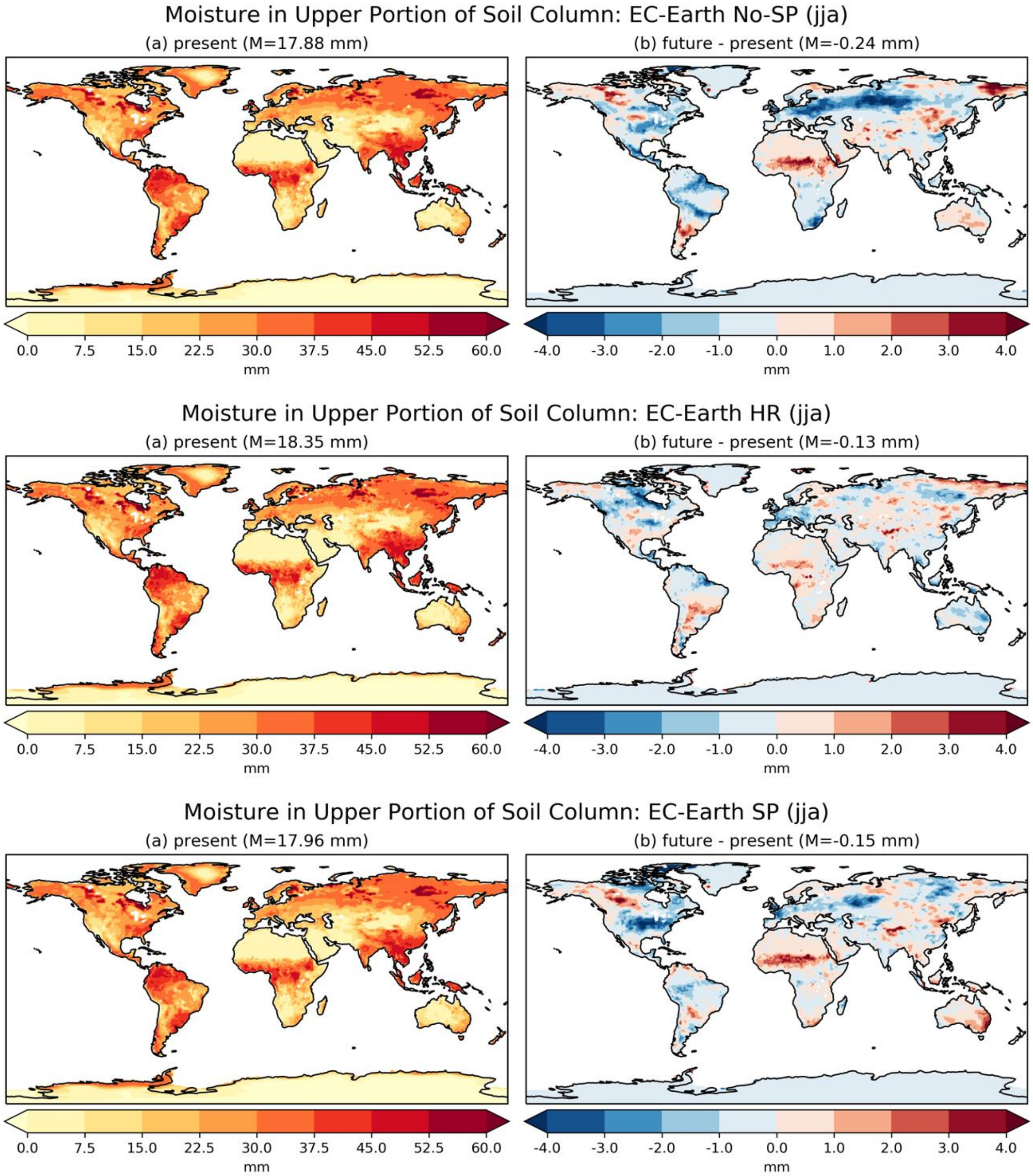

Figure 3.3.7 Future changes to monthly mean soil moisture. JJA only. Top: EC-Earth No-SP, Middle: EC-Earth HR, Bottom: EC-Earth SP. In (a) is shown the present day mean (2000-2014) and (b) is shown future (2036 to 2050) minus present day climate.

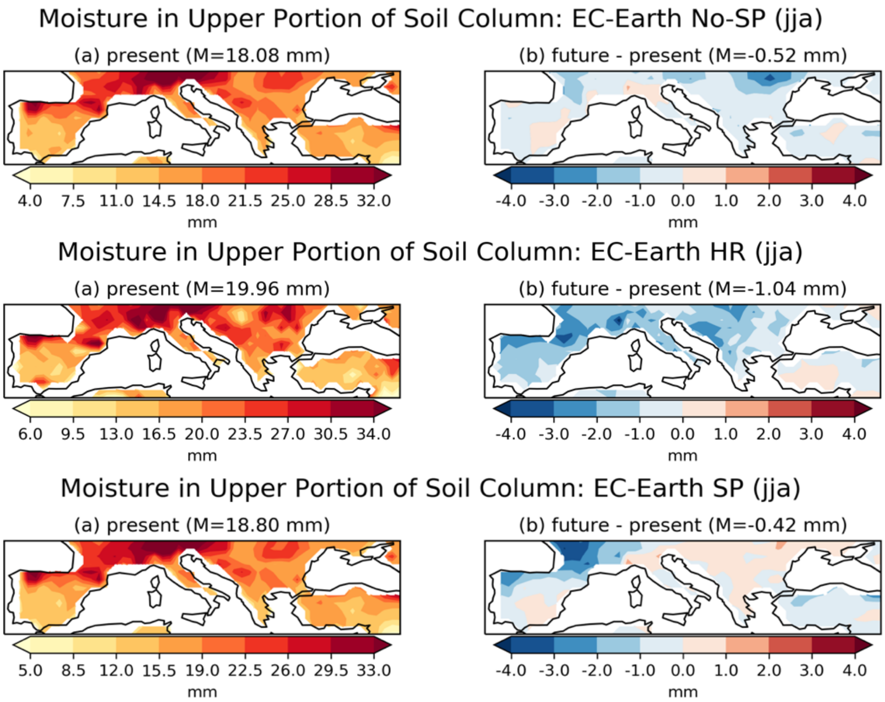

Figure 3.3.8 Future changes to monthly mean soil moisture for Southern Europe. JJA only. Top: EC-Earth No-SP, Middle: EC-Earth HR, Bottom: EC-Earth SP. In (a) is shown the present day mean (2000-2014) and (b) is shown future (2036 to 2050) minus present day climate.

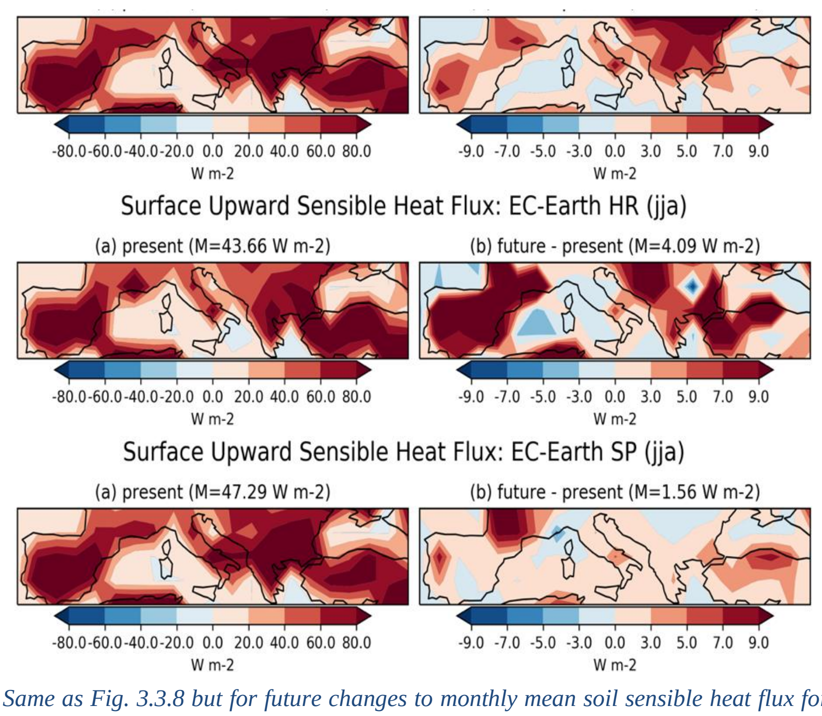

Figure 3.3.9 Same as Fig. 3.3.8 but for future changes to monthly mean soil sensible heat flux for Southern Europe JJA only.

4. Lessons Learnt/ Future directions

As described in this report the precipitation diurnal cycle phase exhibits little sensitivity to the model resolution, for model resolutions which are currently plausible for long climate model integrations (i.e. ~50-100km). Furthermore, it is found that biases in the phase of the diurnal cycle cannot be reduced by the use of stochastic physics. In contrast, high sensitivity of the diurnal cycle phase is found when explicitly treating rather than parametrising deep-convection. In IFS, the main improvement of explicitly representing deep convection comes from the increase in night-time convection, while the daytime onset can even occur earlier or might be delayed compared to the parametrized convection, depending on resolution. Realistically resolving deep convection will require resolutions of 1-2 km, which is currently not feasible for century long model integrations such as those conducted within CMIP - such simulations may also require considerable retuning compared to parameterised models. In contrast, the diurnal cycle amplitude does change with increased resolution (80km → 40km) and with stochastic physics. This suggests that use of stochastic physics might be a computationally cheap way to improve the diurnal cycle amplitude to some extent.

For future projections, it was found that changes in heat fluxes and soil moisture are strongly coupled to changes in precipitation, as expected. Because changes in precipitation were found to be linked, in many cases, to changes in the diurnal cycle amplitude, it is possible that biases in the diurnal cycle are influencing projections of soil moisture, heat fluxes and precipitation, with potential implications for high impact events such as heat waves and drought. Another important lesson was that experiments which performed similarly in the historical period diverged notably in the future, suggesting that the uncertainty associated with unresolved subgrid-scale variability permeates up to uncertainties in the large-scale variability. An important conclusion is that a robust assessment of the relevant uncertainties associated with the diurnal cycle may be needed to obtain more reliable climate projections.

It should be noted that most of the results presented in this deliverable report are based on EC-Earth simulations only. This has been motivated by the fact that all simulations have been available to analyse the effect of both: stochastic physics and resolution. However, in future the analyses should be expanded to other models to also assess the sensitivity of the diurnal cycle characteristics to e.g. different deep-convection schemes. Also, simulations using stochastic physics in other models than EC-Earth are needed to verify in how far improvements in the diurnal cycle amplitude are robust across different models. Furthermore, analyses using a larger ensemble are needed to assess near-future precipitation projections, as changes on the time-scales are substantially affected by internal variability.

Further comparison between global models and regional convection-permitting models (CPMs), where model resolutions can extend to 1-3km scales, could also help to understand the role of large-scale driving compared to local convective influences. However, as in Berthou et al. (2018), plenty of biases and uncertainty remain at such resolutions.

References

Bechtold, P., Semane, N., Lopez, P., Chaboureau, J.-P., Beljaars, A. and Bormann, N. (2014). Representing equilibrium and non-equilibrium convection in large-scale models. J. Atmos. Sci., 71, 734–753.

Birch, C.E., Roberts, M.J., Garcia-Carreras, L., Ackerley, D., Reeder, M.J., Lock, A.P. and Schiemann, R. (2015). Sea-Breeze Dynamics and Convection Initiation: The Influence of Convective Parameterization in Weather and Climate Model Biases. J. Climate, 28, 8093–8108, https://doi.org/10.1175/JCLI-D-14-00850.1

Berthou, S., Kendon, E.J., Chan, S.C. et al. Pan-European climate at convection-permitting scale: a model intercomparison study. Clim Dyn (2018). https://doi.org/10.1007/s00382-018-4114-6.

Buizza, R., Miller, M.J., Palmer T.N. (1999). Stochastic representation of model uncertainties in the ECMWF ensemble prediction system. Q. J. R. Meteorol. Soc., 125, 2887– 2908.

Field, P.R., Roberts, M.J. and Wilkinson, J.M. (2018). Simulated lightning in a convection permitting global model. *Journal of Geophysical Research: Atmospheres*, 123, 9370– 9377. https://doi.org/10.1029/2018JD029295

Huffman, G.J., Bolvin, D.T., Nelkin, E.J., Wolff, D.B., Adler, R.F., Gu, G. Hong, Y. Bowman, K.P. and Stocker, E.F. (2007). The TRMM Multisatellite Precipitation Analysis (TMPA): Quasi-Global, Multiyear, Combined-Sensor Precipitation Estimates at Fine Scales. J. Hydrometeor., 8, 38–55, https://doi.org/10.1175/JHM560.1

Jin, E. K., Choi, I.-J., Kim, S.-Y., and Han, J.-Y. (2016). Impact of model resolution on the simulation of diurnal variations of precipitation over East Asia, J. Geophys. Res. Atmos., 121, 1652– 1670, doi:10.1002/2015JD023948.

Juricke, S., Palmer, T. N., Zanna, L. (2017). Stochastic sub-grid scale ocean mixing: Impacts on low frequency variability. Journal of Climate, JCLI-D-16-0539.1. https://doi.org/10.1175/JCLI-D-16-0539.1

Juricke, S., & Jung, T. (2014). Influence of stochastic sea ice parametrization on climate and the role of atmosphere-sea ice-ocean interaction. Philosophical Transactions of the Royal Society A: Mathematical, Physical and Engineering Sciences, 372(2018). https://doi.org/10.1098/rsta.2013.0283

Love, B.S., Matthews, A.J. and Lister, G.M.S. (2011). The diurnal cycle of precipitation over the Maritime Continent in a high-resolution atmospheric model. Q.J.R. Meteorol. Soc., 137: 934-947. doi:10.1002/qj.809

Palmer T.N., Buizza R., Doblas-Reyes F., Jung T., Leutbecher M., Shutts G.J., Steinheimer, M. and Weisheimer, A. (2009). Stochastic Parametrization and Model Uncertainty. Technical Memorandum 598. ECMWF: Reading, UK.

Sato,T (2008). Resolution Dependency of the Diurnal Cycle of Convective Clouds over the Tibetan Plateau in a Mesoscale Model. Journal of the Meteorological Society of Japan. Ser. II

Strommen, K., Christensen, H. M., Macleod, D., Juricke, S., and Palmer, T.N. (2019). Progress towards a probabilistic Earth system model: Examining the impact of stochasticity in the atmosphere and land component of EC-Earth v3.2. Geoscientific Model Development. https://doi.org/10.5194/gmd-12-3099-2019

Yashiro, H., Kajikawa, Y., Miyamoto, Y. Yamaura, T., Yoshida, R. and Tomita, H. (2016). Resolution dependence of the diurnal cycle of precipitation simulated by a global cloud system resolving model, SOLA, 12, 272–276, doi:10.2151/sola.2016-053.

Model	Ens. Mem.	Years	Temp. res.	Hor. res.	Used in Section
EC-EARTH LR (3P)	1	2000-2014	3hr	TL255	3.1.1, 3.2, 3.3
EC-EARTH LR (3P)	1	2035-2049	3hr	TL255	3.1.1, 3.2, 3.3
EC-EARTH HR (3P_HR)	1	2000-2014	3hr	TL511	3.1.1, 3.2, 3.3
EC-EARTH HR (3P_HR)	1	2035-2049	3hr	TL511	3.1.1, 3.2, 3.3
EC-Earth No-SP	1	2000-2014	3hr	TL255	3.1.2, 3.2, 3.3
EC-Earth SP	1	2035-2049	3hr	TL255	3.1.2, 3.2, 3.3
EC-Earth No-SP	1	2000-2014	3hr	TL255	3.1.2, 3.2, 3.3
EC-Earth SP	1	2035-2049	3hr	TL255	3.1.2, 3.2, 3.3
ECMWF-IFS-4km (w/ conv. parameterization)	1	Aug. 2016	1hr	4km	3.1.3
ECMWF-IFS-4km (w/o conv. parameterization)	1	Aug. 2016	1hr	4km	3.1.3
HadGEM3-GC31-10km (w/ conv. parameterization, CAPE timescale 3600s)	3	2005-2009	1hr	10km	3.1.3
HadGEM3-GC31-10km (no conv. parameterization, prognostic graupel)	1	2005-2009	1hr	10km	3.1.3
HadGEM3-GC31-10km (no deep conv. parameterization, CAPE timescale 5400s)	1	2005-2009	1hr	10km	3.1.3

Table 1 Datasets used in this deliverable report.